

# S.NEST | An intelligent tool with real-time dissolved oxygen and pH monitoring on batch cultures

Hsiao-Ju (Sharon) Chiu, MS, Yan-Ning (Lina) Yu, BS, Shih-Pei (Betty) Lin, PhD  
CYTENA Bioprocess Solutions, Taipei City, Taiwan



## Abstract

Cell growth measurement and metabolism analysis in high-throughput cell culture is a labor-intensive and time-consuming process. Here, we introduced CYTENA BPS's high-throughput microbioreactor, the S.NEST™, and demonstrated the reliability of real-time monitoring functions of dissolved oxygen (DO) and pH. The DO value was correlated with doubling time and cell viability while the pH value was related to cell metabolism and carbon resource utilization. By using the S.NEST to assess DO and pH, the cell growth and metabolic profile could be predicted without any

disturbance. The device could increase the efficiency for cell culture and provide a great platform for process development.

## Introduction

Assessments of cell growth and viability are widely used indicators for mammalian cell culture processes. Advances in technology have made automated instruments for offline cell monitoring a possibility, saving researchers more time compared to manually counting cells with a hemocytometer under microscopy. However, the offline measuring method is inefficient and inadequate for high throughput or continuous culture. Therefore, realtime monitoring methods have been implemented, including laser turbidity, oxygen uptake rate (OUR), dissolved oxygen (DO) and pH level assessment [1].

Measurements of DO and pH levels have been widely used in bioreactors for online monitoring. It is necessary for the control and analysis of cell growth and metabolism. The DO level will decrease with the increasing biomass, which is related to cell respiration and OUR. With more CO<sub>2</sub> and lactic acid generated from cell respiration and glucose metabolism, pH level will decrease. These two process parameters are crucial indicators for cell assessment and have been widely equipped in large-scale culturing platforms, including shake flask and bioreactors. However, it is labor intensive and time consuming to conduct hundreds of experiments on large-scale culturing systems for optimizing manufacturing process [2,3]. The S.NEST microbioreactor was developed to address these challenges by providing powerful realtime monitoring at a smaller scale.

The S.NEST serves as a next-generation microbioreactor. It has four incubation chambers, each composed of thermal modules, water trays, humidity and CO<sub>2</sub> sensors to control the environment independently (**Figure 1A**). Cells can be cultured in a mixing mode with the S.NEST lid. The 24-well fluidic channels from the S.NEST lid could homogenize the culture medium through pneumatic mixing (**Figure 1B**). The S.NEST monitors DO and pH via optical sensor spots, which are fixed to the bottom of the microplate (**Figure 1C**).

With fluorometric sensor tags attached to the bottom of the microplate, measurement of process parameters can be taken in each well simultaneously. The optical sensor is advantageous for its fast detection without interfering or being destructive to the cells. The sensor plate is disposable to prevent cross contamination and is miniaturized with high precision and low cost. Since the DO and pH sensors are not a direct method for cell growth and viability measurement, it is crucial to investigate the relationship and reliability of the two process parameters.

In this study, different densities of Chinese Hamster Ovary (CHO-S) cells were seeded in a 24-well sensor plate to monitor DO and pH in the S.NEST system. We demonstrated that the cell growth and metabolism with different seeding densities were correlated to the DO and pH curves and could be reliable indicators for cell health assessment.

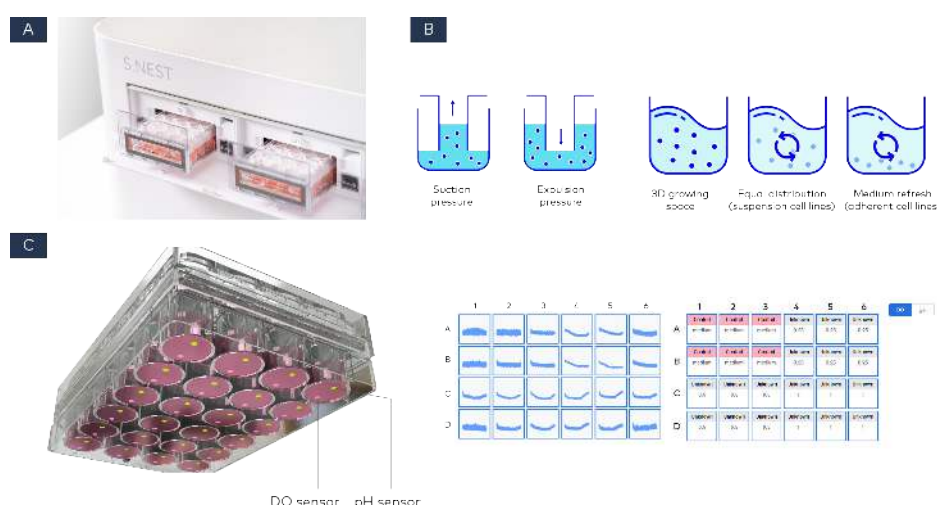


**Figure 1.** (A) The S.NEST culture system contains 4 independent chambers for static or mixing culture. (B) The S.NEST lid provides reciprocal mixing to make medium more homogenous. (C) The S.NEST system provides a real-time monitoring function for DO and pH. The sensor spots were attached to the bottom of the microplates for monitoring.

## Materials and methods

### Cell culture

A monoclonal antibody expressing CHO-S cell line was cultured in CD Hybridoma Medium (Thermo Fisher Scientific, Gibco, #11279023) supplemented with 100 units/mL of penicillin, 100 µg/mL of streptomycin (Thermo Fisher Scientific, Gibco, #5140122), 1X cholesterol lipid concentrate (Thermo Fisher Scientific, Gibco, #12531018), 0.2% anticlumping agent (Thermo Fisher Scientific, Gibco, #0010057DG) and 8 mM L-glutamine (Corning, 25-005-CI). CHO-S cells were passaged every 3 to 4 days and cultured in a humidified incubator with 5% CO<sub>2</sub> and 37°C.

### Mixing culture with different cell seeding density

CHO-S cells were prepared in 2.5x10<sup>5</sup> cells/mL, 5x10<sup>5</sup> cells/mL and 1x10<sup>6</sup> cells/mL for cell seeding. Each density of cells was added to 6 wells of 24-well sensor plate (CYTEAN BPS, #PX24A003) and medium was added to the other 6 wells as control. 18 mL of Dulbecco's phosphate-buffered saline (DPBS) (GeneDireX, #CC702-0500) was added to the inter-well to avoid high evaporation. Cells were cultured in the S.NEST with a 10 seconds/cycle mixing rate for 8 days. The pH and DO sensor spots in the microplate were detected by the camera module equipped in the S.NEST system and the data was collected every 5 minutes. Cell density and viability were counted with an automated cell counter (CURIOSIS, #FACSCOPE) every 2 days.

### Glucose and lactate assay

A glucose assay kit (Abcam, #65333) and L-lactate assay kit (Abcam, #65330) were used to assess cell metabolism. The supernatants, which were collected on day 0, 2, 4, 6 and 8, were diluted from 10 to 200 folds with the kit buffer. The diluted samples and standards were added to the microplate (Corning, #3599) at a 1:1 ratio and incubated at room temperature for 30 minutes in the dark. The absorbance was measured with optical density 570 nm by the microplate reader (Molecular Devices, SpectraMax iD3).

## Results and discussion

### Real-time monitoring and cell measurement

DO and pH play a pivotal role in reflecting cell physiological status. Real-time monitoring of DO and pH from the optical sensor could solve the problem of relatively high costs and contamination risks from the traditional electrochemical principal device. Therefore, validating the reliability of the optical sensors used in a complex biological environment becomes a crucial issue.

Here, cells were seeded with 2.5 x10<sup>5</sup> cells/mL, 5 x10<sup>5</sup> cells/mL and 1x10<sup>6</sup> cells/mL in a 24-well sensor plate and the medium was added as a control (**Figure 2A**). DO and pH were monitored for 8 days. We found that there were two turning points in each DO and pH curve. The DO and pH curves in each group were decreased at the beginning (**Figure 2A**). The decreasing performance of each DO and pH group was correlated to the cell density. The decreasing tendency of DO and pH with higher seeding density was greater than the group with lower seeding density (**Figure 2A**). At the first turning point, the decreasing DO and pH curves flattened, potentially due to the change in the cell growth profile and cell metabolism. At the end of the culture period, the second turning point was observed that the DO and pH curves in each group showed an increasing tendency which was positively correlated to the cell seeding density (**Figure 2A**). To examine if DO and pH curve were related to cell growth profiles, cell growth and viability were also measured.

Cells with a higher seeding density had higher total cell density (TCD) and viable cell density (VCD) but showed lower viability at the end of the culture period (**Figure 2B**). The doubling time was analyzed as 41, 102 and 136 hours in 2.5x10<sup>5</sup> cells/mL, 5x10<sup>5</sup> cells/mL and 1x10<sup>6</sup> cells/mL seeding groups on day 4, respectively (**Figure 2B**). Since the two turning points were observed in the DO and pH curves, the relation between the turning points, the cell growth profiles and metabolism were further investigated.

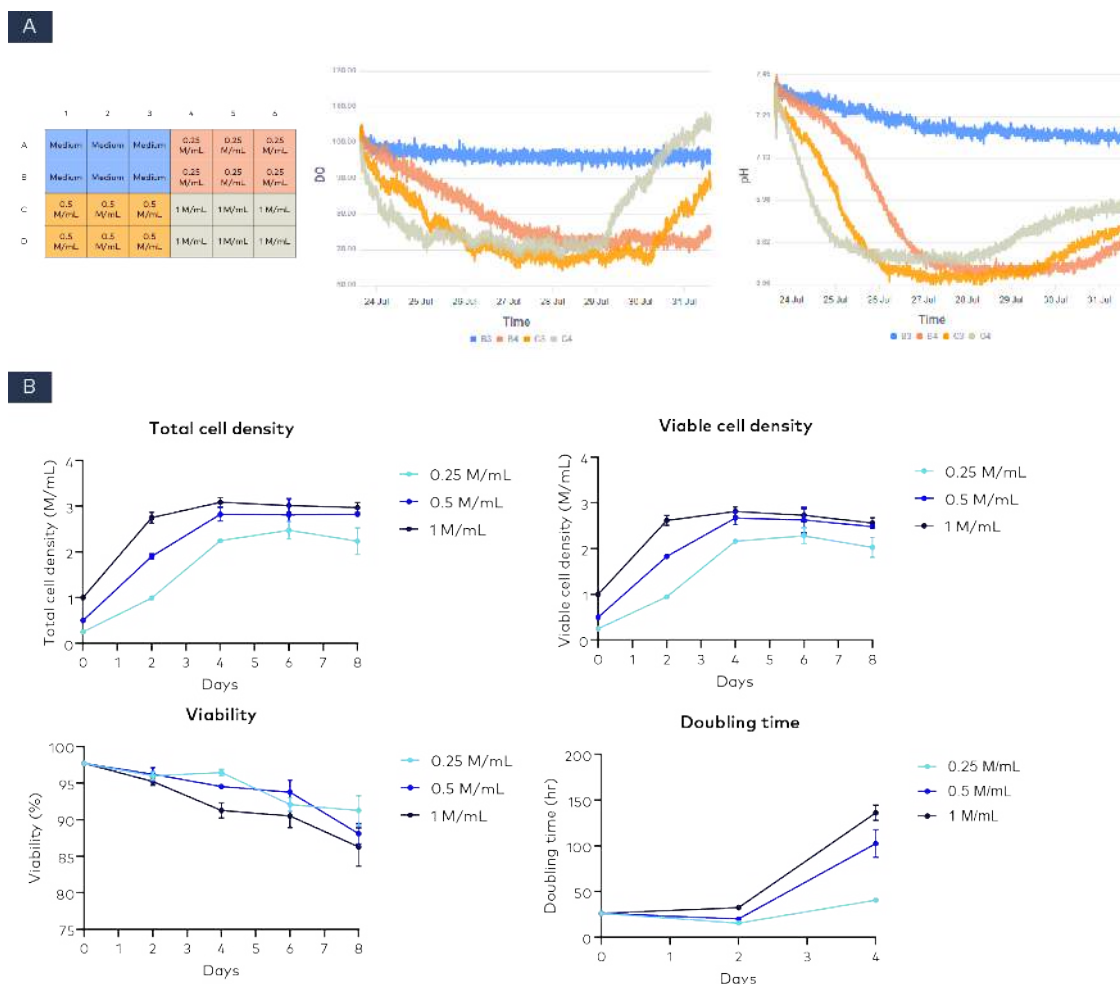


**Figure 2. (A)** Schematic diagram of cell seeding position with different cell seeding densities in the microplate. The representative data of DO and pH curves with different cell seeding densities. **(B)** The total cell density, viable cell density, viability and doubling time were measured and analyzed each 2 days. Data are shown as mean  $\pm$  SEM.

### Glucose and lactate assay

The DO value was related to OUR from the cells and oxygen transfer rate (OTR) from the S.NEST mixing. Since the mixing rate, volume and the culture platform were the same in each seeding density group, OUR became a major influence on the DO value in this application note. Therefore, the two turning points in each cell group were compared with cell physiology. We found that the DO value was decreased to about 80% and the cell doubling time was about 30 hours (**Figure 3A-C**). The DO value of the first turning point in the  $1 \times 10^6$  cells/mL cell seeding density group was measured as 80.75% on day 1.4 and the doubling time was 30.51 hours (**Figure 3A**). The DO value of the first turning point in the  $5 \times 10^5$  cells/mL cell seeding density group was measured as 77.38% on day 2.6 and the doubling time was 44.75 hours (**Figure 3B**).

The DO value of the first turning point in the  $2.5 \times 10^5$  cells/mL cell seeding density group was measured as 76.50% on day 3.5 and the doubling time was 34.35 hours (**Figure 3C**). We found that the DO value started to increase when cell viability was decreased to about 90% (**Figure 3D-F**). The second turning point was observed on day 5.6 in the  $1 \times 10^6$  cells/mL seeding group; viability was decreased to 90.7% (**Figure 3D**). The second turning point was observed on day 6.6 in the  $5 \times 10^5$  cells/mL seeding group; viability was decreased to 92.1% (**Figure 3E**). The second turning point was observed on day 7.4 in the  $2.5 \times 10^5$  cells/mL seeding group; viability was decreased to 91.5% (**Figure 3F**).

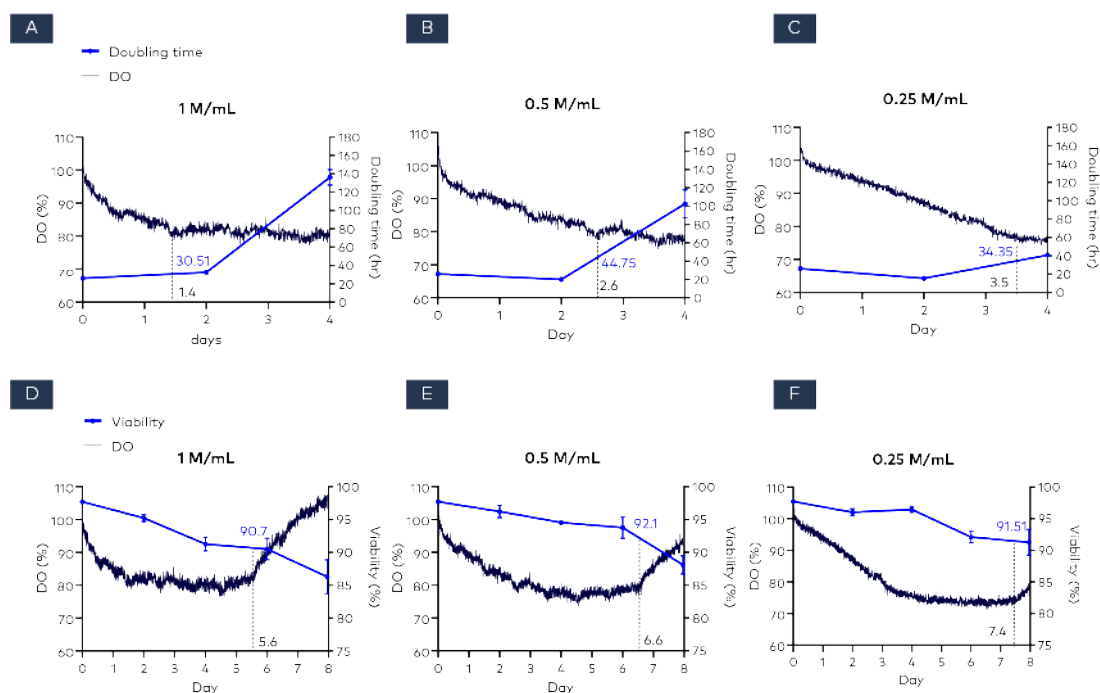


**Figure 3. (A-C)** The first turning point in the DO curves with different seeding densities were analyzed with doubling time. **(D-F)** The second turning point of DO was analyzed and compared with cell viability. All data were shown as mean  $\pm$  SEM.

### Glucose and lactate assay

The main factor that affects pH value in the culture media is cell metabolism. Thus, glucose and lactate assays were conducted to examine cell metabolism in different groups. All groups showed decreasing pH and was correlated to the increasing lactate at the beginning of the culture period until the pH value reached about 6.8 (**Figure 4**). The pH value of the first turning point in the  $1 \times 10^6$  cells/mL cell seeding group was about 6.81 on day 1.6 and glucose and lactate were measured as 1.73 g/L and 1.78 g/L, respectively (**Figure 4A**). The first pH turning point in the  $5 \times 10^5$  cells/mL seeding group was about 6.73 on day 2.6 and glucose and lactate were measured as 1.80 g/L and 1.84 g/L, respectively (**Figure 4B**). The first pH turning point in the  $2.5 \times 10^5$  cells/mL seeding group was assessed as 6.83 on day 3.7 and glucose and lactate were analyzed as 1.36 g/L and 1.63 g/L, respectively (**Figure 4C**). All the seeding group was observed that the first turning point occurred when glucose

concentration was decreased to 0.5-fold of initial glucose concentration and lactate was increased to about 1.75 g/L (**Figure 4A-C**), indicating a potential feeding time point in fed-batch culture. The second turning point was observed at the end of the culture period and was related to metabolism switch. The glucose was almost completely used by the cells and lactate became the main carbon source for cell utilization (**Figure 4D-F**). The second pH turning point of the  $1 \times 10^6$  cells/mL seeding group was measured as 6.75 on day 4.6 and glucose and lactate were assessed as 0.91 g/L and 2.28 g/L, respectively (**Figure 4D**). The second turning point of pH in the  $5 \times 10^5$  cells/mL seeding group was monitored as 6.72 on day 5.6 and the concentration of glucose and lactate was measured as 0.20 g/L and 2.54 g/L, respectively (**Figure 4E**). The second turning point of the  $2.5 \times 10^5$  cells/mL seeding group was observed as 6.8 on day 6.6 and glucose and lactate were shown as 0.06 g/L and 2.28 g/L, respectively (**Figure 4F**).

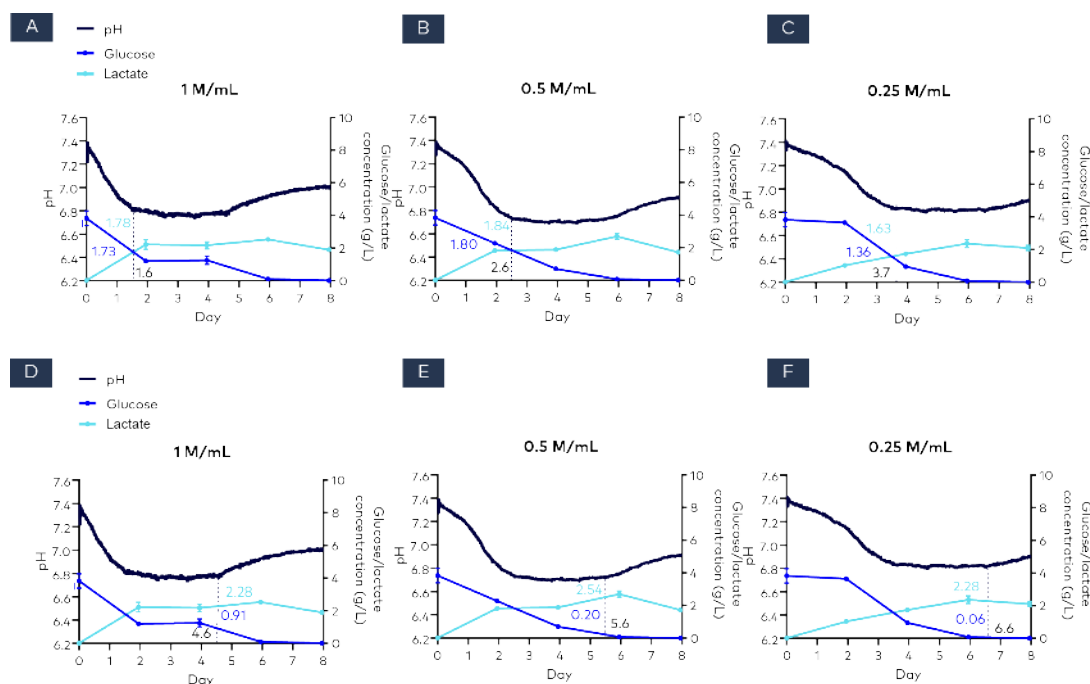


**Figure 4.** The pH was affected by cell metabolism. Part of the media were collected to analyze glucose and lactate concentration. **(A-C)** The first turning point of pH curves was related to the glucose and lactate concentration. **(D-F)** The second turning point of pH curves was related to metabolism switch. All data were shown as mean  $\pm$  SEM.

## Conclusion

Microbioreactor is a highly-utilized and critical system in the upstream processes of CLD workflows including clone selection, batch/fed-batch culture, and media optimization, for example. Though advanced methods are developed to control and monitor process parameters in microbioreactors, the effects of those parameters on cell conditions are still not fully understood. In this study, we demonstrated the significance of DO and pH values for the assessment of growth kinetics and cell metabolism without sampling and showed the reliability of the S.NEST culture system in the meanwhile. Our previous application note showed that our microbioreactor, the C.BIRD, could optimize CLD workflows [4]. Likewise, huge values could be added if a DO and pH monitoring capable system is applied to the CLD workflow during the top-performed clone selection and other dynamic processes such as high-productivity cell culture process development. The DO and pH value monitored from the 24-well microplate served as a basis for later cultivation in a large-scale bioreactor with the aim of optimizing growth kinetics and cell activity. In addition to optimizing CLD, the

S.NEST culture system shows great potential in streamlining the T-cell expansion manufacturing process and pH-sensitive drug pharmacokinetics [5, 6]. The high-throughput characteristic of the S.NEST combined with a statistical tool, such as the Design of Experiment methodology, shows tremendous promise in optimizing process parameters in process development.

## References

1. Naciri M, Kuystermans D, Al-Rubeai M. Monitoring pH and dissolved oxygen in mammalian cell culture using optical sensors. *Cytotechnology*. 2008; 57(3): 245-50. [DOI: 10.1007/s10616-008-9160-1](https://doi.org/10.1007/s10616-008-9160-1)
2. Chen A, Chitta R, Chang D, Amanullah A. Twenty-four well plate miniature bioreactor system as a scale-down model for cell culture process development. *Biotechnology and Bioengineering*. 2009; 102(1): 148-60. [DOI: 10.1002/bit.22031](https://doi.org/10.1002/bit.22031)
3. Hanson MA, Ge X, Kostov Y, et al. Comparisons of optical pH and dissolved oxygen sensors with traditional electrochemical probes during mammalian cell culture. *Biotechnology and Bioengineering*. 2007; 97(4): 833-41. [DOI: 10.1002/bit.21320](https://doi.org/10.1002/bit.21320)
4. Yu N, Chiu S, Lin S. C.BIRD: improving the single-cell cloning workflow through increasing cell growth rate by C.BIRD mixing culture. *www.cytene-bps.com*. 2022. [CBSAPP13](#).
5. Amini A, Wiegmann V, Patel H, et al. Bioprocess considerations for T-cell therapy: Investigating the impact of agitation, dissolved oxygen, and pH on T-cell expansion and differentiation. *Biotechnology and Bioengineering*. 2020; 117(10): 3018-3028. [DOI: 10.1002/bit.27468](https://doi.org/10.1002/bit.27468)
6. Wang Z, Deng X, Ding J, et al. Mechanisms of drug release in pH-sensitive micelles for tumour targeted drug delivery system: A review. *International Journal of Pharmaceutics*. 2018; 535(1-2): 253-260. [DOI: 10.1016/j.ijpharm.2017.11.003](https://doi.org/10.1016/j.ijpharm.2017.11.003)





©2023 BICO AB. All rights reserved. Duplication and/or reproduction of all or any portion of this document without the express written consent of BICO is strictly forbidden. Nothing contained herein shall constitute any warranty, express or implied, as to the performance of any products described herein. Any and all warranties applicable to any products are set forth in the applicable terms and conditions of sale accompanying the purchase of such product. BICO provides no warranty and hereby disclaims any and all warranties as to the use of any third-party products or protocols described herein. The use of products described herein is subject to certain restrictions as set forth in the applicable terms and conditions of sale accompanying the purchase of such product. BICO may refer to the products or services offered by other companies by their brand name or company name solely for clarity and does not claim any rights to those third-party marks or names. BICO products may be covered by one or more patents. The use of products described herein is subject to BICO's terms and conditions of sale and such other terms that have been agreed to in writing between BICO and user. All products and services described herein are intended FOR RESEARCH USE ONLY and NOT FOR USE IN DIAGNOSTIC PROCEDURES.

The use of BICO products in practicing the methods set forth herein has not been validated by BICO, and such nonvalidated use is NOT COVERED BY BICO'S STANDARD WARRANTY, AND BICO HEREBY DISCLAIMS ANY AND ALL WARRANTIES FOR SUCH USE. Nothing in this document should be construed as altering, waiving or amending in any manner BICO's terms and conditions of sale for the instruments, consumables or software mentioned, including without limitation such terms and conditions relating to certain use restrictions, limited license, warranty and limitation of liability, and nothing in this document shall be deemed to be Documentation, as that term is set forth in such terms and conditions of sale. Nothing in this document shall be construed as any representation by BICO that it currently or will at any time in the future offer or in any way support any application set forth herein.

Edited version: September 2023 | CBS\_PUB\_SNEST\_App-Note-16\_Digital